Chinese Journal of Structural Chemistry

REVIEW

Conductive Metal/Covalent Organic Frameworks for CO_2 Electroreduction

Chang-Pu Wan[1,2], Jun-Dong Yi[1,3], Rong Cao[1,2,4]* and Yuan-Biao Huang[1,2]*

[1]*State Key Laboratory of Structural Chemistry, Fujian Institute of Research on the Structure of Matter, Chinese Academy of Sciences, Fuzhou 350002, China*

[2]*University of Chinese Academy of Sciences, Beijing 100049, China*

[3]*School of Chemistry and Materials Science, Collaborative Innovation Center of Chemistry for Energy Materials (iChEM), University of Science and Technology of China, Hefei 230026, China*

[4]*Fujian Science & Technology Innovation Laboratory for Optoelectronic Information of China, Fuzhou 350108, China*

ABSTRACT Porous crystalline metal-organic frameworks (MOFs) and covalent organic frameworks (COFs) are promising platforms for electrocatalytic reduction of CO_2 (CO_2RR) due to their large CO_2 adsorption uptakes and periodically arranged single active sites. However, the applications in CO_2RR of the traditional MOFs and COFs are greatly limited by their low electron conductivity. In recent years, numerous types of MOFs and COFs with high intrinsic conductivity have been rationally designed and successfully constructed, and some of them have been applied in CO_2RR. In this review, the applications of conductive MOFs and COFs in CO_2RR have been summarized. The conductive MOFs and COFs can be categorized according to the methods, in which the conductivity is enhanced, such as constructing fully π-conjugated backbones, donor-acceptor heterojunction, enhancing the π-π stacking interactions between organic moieties and/or the introduction of guest molecules.

Keywords: metal-organic frameworks, covalent organic frameworks, CO_2 electroreduction reaction, conductive frameworks

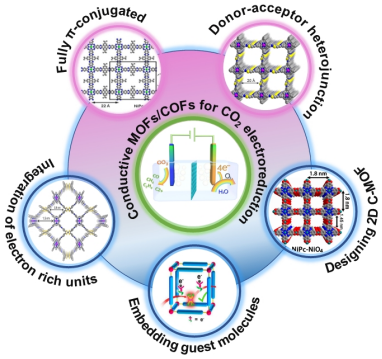

n INTRODUCTION

The excessive utilization of fossil fuels has resulted in high emission of carbon dioxide (CO_2), thus various environmental problems including the rising of sea level, global warning, ocean storms, and increased desertification area. During the past decades, many countries have devoted to finding new green energy sources and renewable sources to replace fossil fuels.[1-3] Although some success has been achieved, there is still a long way to go before conventional fossil fuels are completely replaced due to cost and technological constraints.[4] Therefore, the immediate priority is to decrease the carbon dioxide concentration in the atmosphere, which might simultaneously mitigate the greenhouse effect or energy crisis.

To date, various CO_2 reduction approaches, including electrochemical, biochemical, photochemical, and thermochemical methods, have been proposed and explored.[5] Among them, the CO_2 electroreduction reaction (CO_2RR) has several advantages including controllable processes by adjusting potentials, minimized chemical consumption and feasibility to scale up. Due to its advantages of high environmental compatibility, simple devices, and low energy consumption,[6-10] the electrocatalytic reduction of CO_2 to valued-added products, such as formic acid (HCOOH), carbon monoxide (CO), methanol (CH_3OH), methane (CH_4), ethylene (C_2H_4) and ethanol (CH_3CH_2OH), is a promising strategy of turning waste into treasure. However, the transformation from the stable linear CO_2 molecule to the bent $CO_2^{\cdot-}$ radical anion requires large reorganization energy, resulting in the high thermodynamic stability.[11] Therefore, it is difficult to activate CO_2, which usually needs large overpotentials. Besides, the thermodynamic redox potentials of these products are close, giving rise to a poor selectivity for a specific product. Thus, if CO_2RR is expected to be a viable option for storing renewable energy, significant hurdles concerning the high energy efficiency and selectivity must be overcome.

Although various physical and chemical processes might be involved, the reaction process of CO_2RR (Figure 1) mainly involves three steps: (1) the adsorption and activation of CO_2 molecules on the surface of electrocatalyst; (2) the breaking of C-O bonds and/or the forming of C-H bonds; (3) the desorption and configuration rearrangement of products. Besides, the associated competing hydrogen evolution reaction (HER) in aqueous medium also should be inhibited in CO_2RR.[12-15] Therefore, exploring appropriate electrocatalysts is of critical importance for CO_2RR.

Nowadays, the electrocatalysts for CO_2RR can be divided into two groups: homogeneous molecular catalysts and heterogeneous catalysts. Compared with heterogeneous catalyst, homogeneous catalyst usually suffers from drawbacks including product isolation, catalyst recovery, and poor stability. Meanwhile, only molecules close to the electrode in the diffusion layer could take part in the reaction process, lowering the utilization of molecules. Therefore, the homogeneous molecular catalysts could not be regarded as an ideal candidate for CO_2RR. On the contrary, the excellent stability of heterogeneous catalysts in water makes them have great potential for CO_2RR, which no longer

DOI: 10.14102/j.cnki.0254-5861.2022-0075

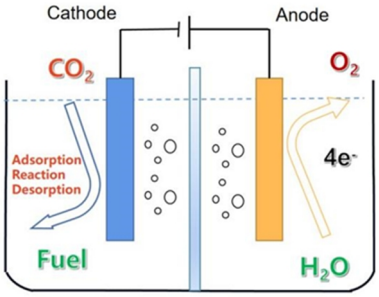

Figure 1. The major reaction process of electrochemical CO_2 reduction.

depends on the diffusion of catalyst and is not limited by the solubility of catalyst.[16-21] Thus, immobilizing homogeneous molecular catalysts into heterogeneous matrixes seems to be a promising way to tackle the above issues. Fortunately, metal-organic frameworks (MOFs) and covalent organic frameworks (COFs) can bridge the gap between homogeneous and heterogeneous catalysis, by integrating active metal complexes into the porous stable organic frameworks, which retains the same highly efficient and accessible active sites of homogeneous catalysts and the recyclable characteristics of heterogeneous catalysts.

In the past decades, porous crystalline MOFs and COFs have been attractive materials in CO_2RR, which are mostly attributed to the adjustable porosity, accessible active sites, large CO_2 adsorption uptakes, periodic metal arrangement and well-defined periodic structure.[22-29] In addition, functional ligands, metal nodes, and active specie can be incorporated in MOFs and COFs for CO_2RR. However, the electrocatalytic activities of most traditional MOFs and COFs are greatly limited by their poor electron conductivity. Therefore, it is very important to improve the intrinsic conductivity of MOFs and COFs to enhance their activity towards CO_2RR. Recently, several types of conductive MOFs and COFs with high intrinsic conductivity have been rationally designed and applied in CO_2RR. Compared with traditional MOFs and COFs, these conductive porous frameworks with better electron conductivity could improve the charge carrier mobility in periodic structures and transfer electrons to active sites and substrate faster, thus showing higher current densities.

There is no doubt that the design and construction of conductive porous crystalline materials are a promising strategy to improve the catalytic performance in CO_2RR. In order to have a better understanding of the superiority of conductive MOFs and COFs, the main body of this review will analyze the catalytic performance of conductive frameworks compared with the traditional MOFs and COFs catalysts. Besides, the synthetic strategy of conductive framework materials will also be summarized. Finally, we will discuss the opportunities and challenges of conductive MOFs and COFs materials as CO_2RR catalysts in the future.

n POOR CONDUCTIVITY MOFS AND COFS CATALYSTS FOR CO_2RR

Compared to traditional solid metal electrodes, the ordered and porous networks in MOFs and COFs allow the ions and dissolved CO_2 to penetrate inside the film. Meantime, the inherent pore confinement properties can induce local CO_2 concentration enhancement, which may allow CO_2RR to catalyze in a diluted CO_2 environment. However, the inherent porosity of MOFs and COF also precludes close intermolecular contacts in many structural types, resulting in low conductivity for these materials. In this section, the MOFs and COFs with poor conductivity regarded as electrocatalysts for CO_2RR are included, aiming to show the differences from conductive MOFs and COFs.

MOF Catalyst with Poor Conductivity. For MOF materials based on active inorganic secondary building units as catalytic centers for CO_2 reduction,[30-36] one copper metal organic framework MOF (CR-MOF) was firstly employed as electrode for CO_2RR in 2012.[30] When tested in 0.5 M $KHCO_3$ aqueous medium, the CR-MOF exhibits a high selectivity over 90% towards formic acid at -1.6 V. vs. reversible hydrogen electrode (RHE). The reason for such high selectivity was ascribed to a decreased electron density of coordinated copper sites in CR-MOF, which may result in a weak interaction of CO_2, thus leading to selective formation of formic acid. Additionally, the onset potential of CR-MOF for CO_2 is also higher than that of metal copper.

And, metalloporphyrins with 2D square geometry have been demonstrated as feasible building blocks for many supramolecular architectures, which possess high thermal stability. Therefore, Hupp and coworkers[31] used the Fe-porphyrin-based MOF (MOF-525) as a platform to anchor a large number of electroactive Fe-porphyrin sites on a conductive electrode for CO_2RR. The approach yields a high effective surface coverage of electrochemically addressable catalytic sites (~1015 sites cm^{-2}). However, when tested in acetonitrile/tetrabutylammonium hexafluorophosphate ($TBAPF_6$) solutions (CO_2-saturated), the current densities of Fe-MOF-525 can only reach 2.3 mA cm^{-2}. Besides, these values correspond to a CO turnover number (TON) of 272 and an average turnover frequency (TOF) of 64 hr^{-1}.

Furthermore, to improve the CO_2RR activity of traditional MOFs, Yang and coworkers[32] demonstrated an atomic layer deposition (ALD)-assisted strategy to fabricate Co-porphyrin based MOF thin films for CO_2RR, in which MOFs grew in situ on the conductive substrate (Figure 2). The ALD-based MOF conversion technique allowed precise control on catalyst loading, enabling the optimization to balance the active-site density with mass/charge transfer. Therefore, they began with 50 ALD cycles of alumina thin films (thickness of 5 nm) deposited onto conductive carbon disk electrodes, and converted the alumina film to porphyrin-containing MOF [$Al_2(OH)_2$TCPP-M'] structures with free-base porphyrin as well as porphyrin centers metalated with M' = Zn, Cu, and Co. Detailed examination of a cobalt-porphyrin MOF revealed a selectivity for CO production in excess of 76%

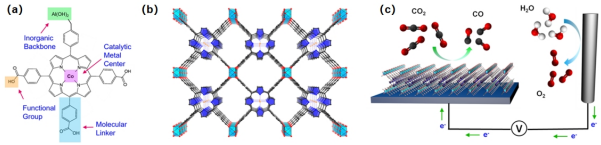

Figure 2. (a) Co-metalated TCPP units. (b) Illustration of the 3D MOF assembly. (c) Functional principles of CO_2RR in the integrated system. Reproduced with permission from Ref.[32]

DOI: 10.14102/j.cnki.0254-5861.2022-0075

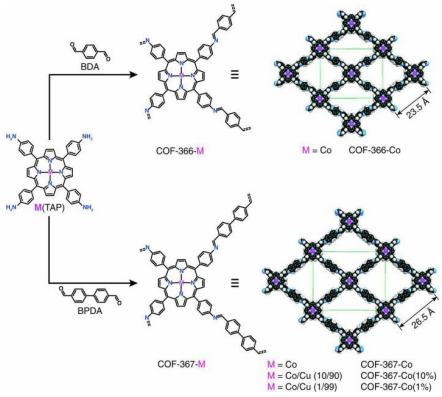

Figure 3. The synthesis of metalloporphyrin-based 2D covalent organic frameworks. Reproduced with permission from Ref.[37]

and stability over 7 h with a per-site TON of 1400. When tested in CO_2-saturated solutions, the current densities of $Al_2(OH)_2$TCPP-Co can reach 5.9 mA cm^{-2}.

COF Catalyst with Poor Conductivity. Compared with MOFs, COFs with imine or amine bonds have more stable structures. Besides, most COF materials are two-dimensional, resulting in many active sites not exposed within the layers, thus mostly exfoliating them ultrasonically into nanosheets to enhance the activity of the catalysts.[37-44] In 2015, Yaghi and coworkers[37] synthesized a 2D COF (COF-366-Co) (Figure 3), in which the cobalt porphyrin sites can catalyze CO_2RR for the conversion of CO_2 to CO. When tested in aqueous solutions, the COF-366-Co showed a high faraday efficiency of CO (FE_{CO}) of 90%, which is 10% higher than the molecular cobalt porphyrin catalyst. At −0.67 V vs. RHE, in accordance with the Co(II)/Co(I) redox potential, the catalyst displayed optimal performances, consistent with former reports that the reduced Co(I)-porphyrins are the active sites for CO_2-to-CO reduction. After continuous controlled potential electrolysis (CPE) for 24 h, TON and an initial TOF of COF-366-Co can reach 34,000 and 2500 h^{-1}, respectively. Although the COF-366-Co resulting from co-facial stacks of porphyrins could act as conduits for the delivery of electrons from the underlying electrode to the many exposed Co sites, the narrow channels inside might hinder the adsorption of carbon dioxide, and thus, there are only few active sites that can be in direct contact with reactants. Fortunately, COFs can introduce topologically identical and functionally modified building blocks to precisely tune their properties. Subsequently, they prepared the expanded COF-367-Co by replacing the 1,4-benzene-dicarboxaldehyde (BDA) strut with biphenyl-4,4′-dicarboxaldehyde (BPDA) (Figure 3). A larger pore size would allow a higher CO_2 adsorption capacity within the framework, leading to an enhancement of the catalytic efficiency. As expected, both smaller overpotential and higher catalytic current density of COF-367 in the CO_2RR were achieved. Compared to COF-366-Co, COF-367-Co exhibits a TON up to 48,000 with a high FE_{CO} of 91%.

In addition to metalloporphyrins, metallopyridine has also been employed as an active building block to introduce into COFs for CO_2RR. In 2018, Marinescu and coworkers[41] integrated Re(2,2'-bpy) $(CO)_3$ fragments into a COF through post-metallation synthetic (Figure 4). Although, Re(2,2'-bpy) $(CO)_3$ reduced CO_2 to CO at -2.57 V vs. ferrocene/ferrocenium with a faradaic efficiency of 99% during 1 hour of electrolysis, the highest FE_{CO} of COF-2,2′-bpy-Re only can reach 81%. The poor electrocatalytic activity of the composite was attributed to poor conductivity and charge transfer.

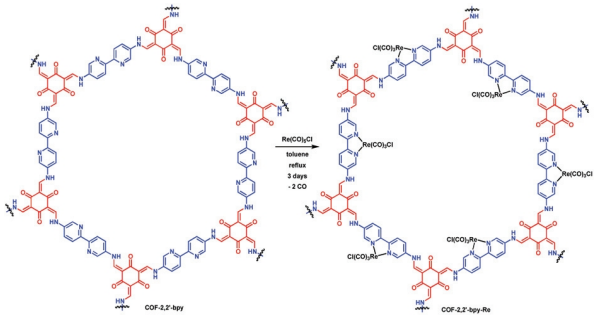

Figure 4. Design and synthesis of Rhenium bipyridine derived covalent organic frameworks. Reproduced with permission from Ref.[41]

n CONDUCTIVE MOFS AND COFS CATALYSTS FOR CO_2RR

As mentioned above, MOFs and COFs with poor electrical conductivity and electron-donating capability are the major constraints for being as efficient electrocatalysts for CO_2RR.[45] Among them, the intrinsic porosity of MOFs and COFs, which makes the intermolecular intimate contact, is the main reason for the low electrical conductivity. Additionally, the majority of MOFs are formed with carboxylate linkers, which usually form relatively ionic bonds with the metals, leading to large energy gaps and trapped valences/confined electronic states. In general, CO_2RR involves three main steps, the chemical adsorption of CO_2 on active sites of electrocatalysts, the multiple protons coupled electron transfer (PCET) to cleave C-O bonds and/or form C-H bonds, and desorption of products from the electrode surface. Notably, the fast electronic transport from electrode to active site and reactants is favorable for achieving high electrocatalytic performance. Thus, the intrinsic conductivity of electrocatalyst is the key parameter for good electrode material. However, majority of MOFs/COFs with poor electrical conductivity usually afford very low current densities and limited energy conversion efficiency in CO_2RR. Hence, it is highly desirable to prepare conductive MOF/COF catalysts with fast electron transfer ability to the integrated single active sites for CO_2RR in order to generate high current density. In this part, we will mainly focus on recent work boosting charge diffusion rates of MOFs or COFs for enhancing CO_2RR.

n CONDUCTIVE MOF CATALYSTS FOR CO_2RR

The design strategies for conductive MOFs are: (1) Some 2D MOFs with π-d conjugation allow for efficient delocalization of charge carriers within the plane, which usually exhibit higher conductivities than 3D MOFs; (2) The integration of electron rich units into MOFs structures will result in the formation of small

DOI: 10.14102/j.cnki.0254-5861.2022-0075

band gaps and high charge mobilities, both of which are favorable for conductivity; (3) The porosity of MOFs can be exploited to induce conductivity by post synthetically loading of electroactive guest molecules into the framework, thus forming charge transport pathways throughout the material through guest-guest or guest-framework interactions.[46-50] Therefore, we will mainly focus on the design and application of conductive MOFs in this section.

Designing 2D Conjugated MOF Catalysts. A large number of active sites inside the 3D MOFs are not effectively utilized during the catalysis due to the presence of diffusion barrier, resulting in low turnover efficiency for CO_2RR. The fabrication of 2D MOFs into ultrathin nanosheets not only allows the control of types of catalytic sites and the micro-environments around it within the thickness of one or several molecular layers, thus maximizing the number of catalytic sites, but also accelerates the mass transport and charge transfer processes.[42,43] Recent studies have found that layered 2D conjugated MOFs (2D c-MOFs) with fully in-plane π-delocalization along 2D directions and weak out-plane π-π stacking exhibited higher density of exposed metal centers and improved electron conductivity up to 2500 S cm^{-1} apart from the inherited features of traditional MOFs.

Recently, Cao and coworkers[42] integrated Ni-phthalocyanine motif (NiPc) into a conductive 2D MOF NiPc-NiO_4 (Figure 5a) highly efficient CO_2RR, and its conductivity can reach up to 4.8 × 10^{-5} S m^{-1} due to the high d-π orbital overlap between the nickel node and the catechol. Besides, after making 2D MOF into nanosheets, the NiPc-NiO_4 nanosheets exhibited a very high selectivity of 98.4% towards the production of CO and a large CO partial current density of 34.5 mA cm^{-2} (Figure 5b, c and d). In addition, the TOF of NiPc-NiO_4 can also reach a maximum of

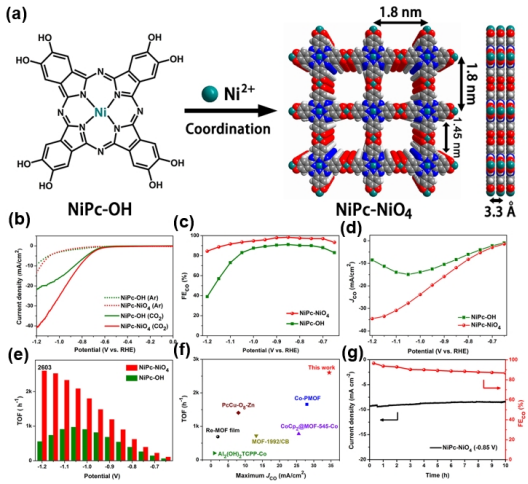

Figure 5. (a) Schematic illustration of the synthesis of two-dimensional NiPc-NiO_4. (b) LSV curves of NiPc-NiO_4 and NiPc-OH in CO_2- and Ar-saturated 0.5 M $KHCO_3$. (c) FE_{CO} at different potentials. (d) CO partial current density, (e) TOF for NiPc-NiO_4 and NiPc-OH. (f) Comparison of the TOF and maximum CO partial current density with reported MOF catalysts. (g) Stability of NiPc-NiO_4 at a potential of -0.85 V vs. RHE for 10 h. Reproduced with permission from Ref.[42]

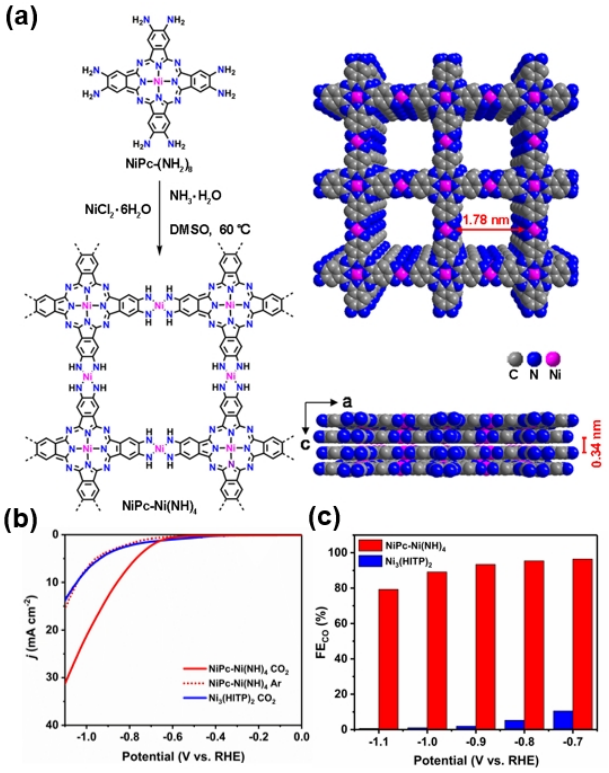

Figure 6. (a) Schematic illustration of the synthesis of two-dimensional NiPc-Ni$(NH)_4$. (b) LSV curves in the Ar- and CO_2-saturated 0.5 M $KHCO_3$ electrolytes at a scan rate of 10 mV s^{-1}. (b) FE_{CO} from -0.7 to -1.1 V of NiPc-Ni$(NH)_4$ and Ni_3(HITP)$_2$. Reproduced with permission from Ref.[43]

2603 h^{-1} at -1.2 V, attributed to its high specific surface area and high conductivity. Such high TOF and CO partial current density are better than many reported MOF catalysts (Figure 5e and f). Besides, a long-term stability test for 10 h at -0.85 V vs. RHE shows that the current density of NiPc-NiO_4 only decreases 0.8 mA cm^{-2}, suggesting good stability of the NiPc-NiO_4 catalyst (Figure 5g).

Besides, Huang and coworkers[43] reported a new conductive 2D COF NiPc-Ni$(NH)_4$, in which the planar NiPc motifs were linked by the Ni$(NH)_4$ nodes (Figure 6a). When tested in aqueous solution, NiPc-Ni$(NH)_4$ exhibited large partial current density of 24.8 mA cm^{-2} for CO_2RR, and the maximum FE_{CO} can reach up to 96.4% at -0.7 V vs. RHE (Figure 6b and c). Overall, this excellent catalytic ability of NiPc-Ni$(NH)_4$ in CO_2RR is attributed to highly electrical conductivity of 2.39 × 10^{-4} S m^{-1} due to the high overlap of d-π conjugation orbitals between the nickel node and the planar Ni-phthalocyanine substituted o-phenylenediamine. Furthermore, the porous NiPc-Ni$(NH)_4$ has a large CO_2 adsorption capacity of 41 cm^3 g^{-1} at 298 K, which suggests a strong CO_2 affinity by the NiPc-Ni$(NH)_4$ with a nitrogen-rich structure for enhancing its electrocatalytic activity in CO_2RR.

In addition to the conductivity of MOFs, Mirica and coworkers[44] found that the catalytic performance of MOFs, including the activity and selectivity, is governed by two important structural factors: the metal within the MPc (M = Co vs. Ni) catalytic

DOI: 10.14102/j.cnki.0254-5861.2022-0075

subunit and the identity of the heteroatomic cross-linkers between these subunits (X = O vs. NH). They focus on the use of four systematic isoreticular structural analogs of 2D conductive MOFs, including CoPc-Cu-NH, CoPc-Cu-O, NiPc-Cu-NH, and NiPc-Cu-O, as electrocatalysts in the electrochemical reduction of CO_2 that permits the modulation of efficiency, activity, and selectivity. These four MOFs share the same lattice with square pore apertures of 1.8 nm with large surface-to-volume ratios and BET surface areas of 349-628 $m^2\ g^{-1}$, good CO_2 adsorption abilities of 1.48-2.03 mmol g^{-1} (900 Torr, 298 K), and good electrical conductivities in the range of 2.73 × 10^{-3} to 1.04 × 10^{-1} S cm^{-1}. Density functional theory (DFT) calculations suggested that, compared with the NiPc-based and NH-linked MOFs, CoPc-based and O-linked MOFs can lower the activation energies in the formation of carboxyl intermediate, thus giving higher activity and selectivity.

In 2020, Feng et.al.[45] developed a layer-stacked, bimetallic 2D c-MOF (PcCu-O_8-Zn) with copper-phthalocyanine as ligand (CuN_4) and zinc-bis(dihydroxy) complex (ZnO_4) as linkage. The PcCu-O_8-Zn exhibits high CO selectivity of 88%, TOF of 0.39 s^{-1} and long-term durability (>10 h). What is more, the spectroscopic studies combined with contrast experiments and DFT calculation reveal that ZnO_4 complexes in the linkages of PcCu-O_8-Zn exhibit high catalytic activity for CO_2-to-CO conversion, while CuN_4 complexes in the Pc macrocycles act as the synergetic component to promote the protonation process and hydrogen generation along with the CO_2RR. For multicarbon products, C-C dimerization is an important step, and optimizing its energy barrier is beneficial for yielding C_2H_4. During CO_2RR, *CHO is believed to be the key intermediate generated. However, the formation of *CHO intermediate needs high adsorption enthalpy, which goes against the desorption of CO, resulting in a high C-C dimerization energy barrier. Therefore, Liao and coworekers[46] reported a 2D MOF PcCu-Cu-O as the electrocatalyst for CO_2 to C_2H_4, by combining the CO- and C_2H_4-producing sites, which can reduce the energy barrier in the C-C dimerization. Meanwhile, the conductivity of PcCu-Cu-O can reach 5 S m^{-1}. This is beneficial for efficient electron transfer in electrocatalysis and yielding hydrocarbons with a high current density.

Furthermore, conductive MOFs also can serve as substrates to anchor active sites in CO_2RR. Recently, Huang and coworkers[47] have designed a 2D conductive Cu-based MOF (MOF-CuHHTP), in which Cu ions in CuHHTP were partially reduced to single-type Cu_2O sites by electrochemical method, giving rise to a highly active electrocatalyst Cu_2O@CuHHTP (Figure 7a). More importantly, the reduction of Cu centers to Cu_2O releases abundant uncoordinated hydroxyl groups near the active sites, which can form hydrogen bonds with intermediates and lower the energy barrier towards the formation of CH_4. When tested in CO_2-saturated electrolyte, the Cu_2O@CuHHTP exhibited outstanding CO_2RR performance with 73% FE of the conversion from CO_2 to CH_4 with partial current density of 10.8 mA cm^{-2} at -1.4 V vs. RHE in CO_2RR (Figure 7b). However, the pristine CuHHTP shows poor CH_4 selectivity, strongly indicating that the CO_2RR activities were originated from Cu_2O quantum dots but not CuHHTP. The electrical conductivity of CuHHTP can reach high value of 5.1 × 10^{-5} S m^{-1} due to the periodically distributed Cu-O_4 nodes in the Cu-based MOF, where the nodes form d-π orbital overlap between the nickel node and the catechol. In addition, the electrical conductivity of Cu_2O@CuHHTP can also reach 4.3 × 10^{-6} S m^{-1}. Therefore, the electrons could be easily transferred to the Cu_2O single-type sites through the conductive CuHHTP substrate, which would be beneficial to expedite the electron transfer during the CO_2RR. Besides, the reduction of Cu centers to Cu_2O releases abundant uncoordinated hydroxyl groups neighboring the active sites, thus forming hydrogen bonds with intermediates and lower the energy barrier towards the formation of CH_4.

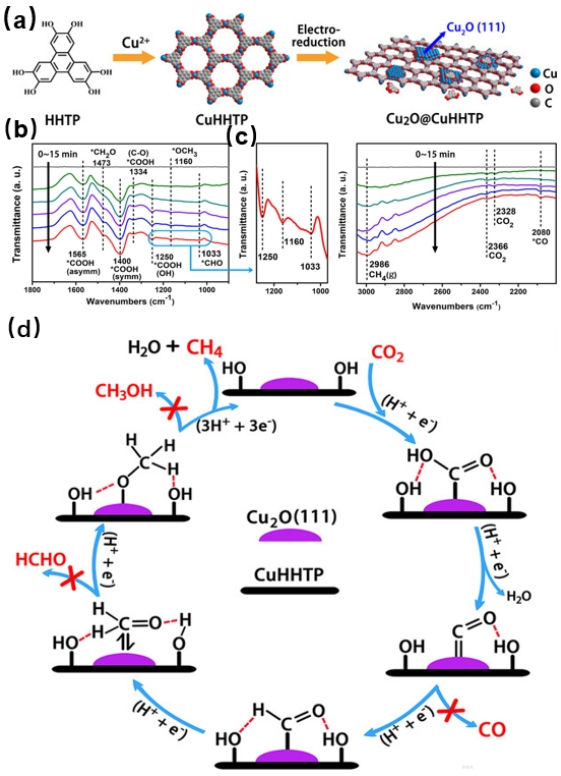

Figure 7. (a) Design and synthesis of Cu_2O@CuHHTP. (b) LSV curves of CuHHTP and Cu_2O@CuHHTP in 0.1 M KCl/0.1 M $KHCO_3$ electrolyte under Ar and CO_2. (c) The free energy diagrams of CO_2 reduction to CH_4 for Cu_2O(111)@HHTP (red line) and pristine Cu_2O(111) crystal plane (black line). (d) Proposed mechanism of Cu_2O@CuHHTP for the formation of CH_4. Reproduced with permission from Ref.[47]

Notably, the CO_2 reduction pathway to produce CH_4 involves eight electron-transfer steps resulting in the generation of at least seven possible intermediates.[46] Based on the operando ATR-FTIR spectra analysis (Figure 7b and c), CO_2 molecules are firstly adsorbed and activated on the (111) crystalline plane of Cu_2O quantum dots, which are quickly transformed into *COOH through a PCET process. The intermediate *COOH could form two hydrogen bonds with the hydroxyl groups of the HHTP ligand. Subsequently, *CO intermediate is generated via a PECT process from the hydrogen bonds-stabilized *COOH intermediate, and simultaneously an equivalent water releases (Figure 7d). A hydrogen bond is also formed between the *CO intermediate and

DOI: 10.14102/j.cnki.0254-5861.2022-0075

Table 1. Comparison of the Highest Current Density, and Faraday Efficiency of Different Conductive MOFs for CO_2RR

Catalysts	The highest J_{CO} (mA cm^{-2})	Electrolyte	The highest FE (%)	Conductivity (S m^{-1})	Ref.
NiPc-NiO_4	34.5 (-1.2 V)	0.5 M $KHCO_3$	98.4 CO (-0.6 V)	4.8×10^{-5}	[42]
NiPc-$Ni(NH)_4$	24.8 (-1.1 V)	0.5 M $KHCO_3$	96.4 CO (-0.7 V)	2.39×10^{-4}	[43]
Co-PMOF	28.5 (-1.1 V)	0.5 M $KHCO_3$	99 CO (-0.8 V)	N.A.	[52]
MCp_2@MOF-545	25.63 (-0.9 V)	0.5 M $KHCO_3$	97 CO (-0.7 V)	1.01×10^{-3}	[55]
CoPc-Cu-O	17.3 (-0.63 V)	0.5 M $KHCO_3$	85 CO (-0.63 V)	1.04×10^{-1}	[44]
PcCu-O_8-Zn	8 (-1.0 V)	0.5 M $KHCO_3$	88 CO (-0.7 V)	N.A.	[45]
PcCu-Cu-O	7.3 (-1.2 V)	0.1 M $KHCO_3$	50 C_2H_4 (-1.2 V)	5	[46]
Cu_2O@CuHHTP	10.8 (-1.4 V)	0.1 M KCl/0.1 M $KHCO_3$	77 CH_4 (-1.4 V)	5.1×10^{-5}	[47]

Note: N.A. means not mentioned in the corresponding literature. All potentials are with reference to the RHE.

the neighboring hydroxyl group of HHTP, therefore hindering the desorption of *CO from the active site to form CO molecule. Besides, the hydrogen bonding interactions between other intermediates and the hydroxyl groups of HHTP could also form and hinder the formation of byproducts like HCHO or CH_3OH, leading to the outstanding selectivity of CH_4 for Cu_2O@CuHHTP. In the following PCET steps, *CHO, *CH_2O and *OCH_3 intermediates generate in turn and are finally reduced to CH_4 and *O, which is reduced to H_2O.

Overall, constructing copper-based electrocatalyst with single type of active site can achieve high selectivity of CH_4.[49-51] Besides, introducing intermolecular interaction with hydrogen bonds in reaction system could stabilize specific intermediate and make the reaction proceed to the expected pathway. Finally, the CuHHTP support accelerates the electron transfer to the active sites and substrate.

Integration of Electron Rich Units. The integration of electron rich units, electron mobility, and active components associated with specific electrocatalytic CO_2 reduction products into MOFs is an effective way to improve the selectivity and efficiency of CO_2RR. In addition, the integration of multifunctional units within MOFs is another promising approach to achieve highly efficient MOFs based strategies due to their easy processing, versatile material selection, and potential to generate highly selective products.

Recently, Lan and coworkers[52] have assembled reductive polyoxometalates (POMs) and metalloporphyrin to construct two-fold interpenetrated mog topology MOFs, which might endow these structures with high chemical, thermal, or catalysis stability. In such PMOFs, Zn-ε-Keggin and metalloporphyrin can serve as the role of gathering electron donating and electron migration in CO_2RR, respectively. Notably, the oriented electron transportation pathway can be created through the connection of POM and metalloporphyrin, when excited by electric field, which might be beneficial for efficient charge transfer. In these PMOFs, Co-PMOF exhibits remarkable faradaic efficiency (> 94%) over a wide potential range (-0.8 to -1.0 V), which is better than other M-PMOFs. To elucidate the dynamic activity of Co-PMOF for electrochemical CO_2RR, the Tafel slope for Co-PMOF is 98 mV dec^{-1}, which is much smaller than that of others. This indicates the favorable kinetics of Co-PMOF for the formation of CO, which might be ascribed to the more efficient charge transfer and larger active surface in the catalytic process. Additionally, the Nyquist plots also indicate Co-PMOF can provide faster electron transfer from the catalyst surface to the reactant (i.e., CO_2) in intermediate (HCOO* and CO*) generation, eventually resulting in largely enhanced activity and selectivity. As a result, its best faradaic efficiency can reach up to 99% and it exhibits a high TOF of 1656 h^{-1} (-0.8 V) and excellent catalysis stability (> 36 h).

To further support the catalytic mechanism of M-PMOF, MOF-525 (Co) was prepared by Hupp and coworkers[53] as relevant comparison which has a similar ligand to the Co-PMOF but without POM. When tested in the same testing methods, the electrochemical CO_2RR of MOF-525(Co) shows lower FE_{CO} (47.9%) than Co-PMOF (98.7) at -0.8V vs. RHE, which might be attributed to the poorer proton and electron transfer efficiency. This indicates POM actually acts as electron-rich aggregates in the catalytic mechanism of M-PMOF. The integration of electron rich units into MOFs greatly enhances the selectivity of CO_2RR. However, it remains challenging to select suitable ligands and electron rich units to construct novel MOFs with high selectivity and efficiency.

Embedding Guest Molecules into MOFs. By leveraging the intrinsic microporosity of MOFs, high loadings of electroactive molecules can be introduced into the pores to increase electrical conductivity. Therefore, Lan and coworkers[54] implant metallocene in MOFs and the thus-obtained catalysts present excellent CO_2RR electrocatalysis performances. Metallocene (MCp_2, Cp stands for cyclopentadienyl) is an electron-rich system with high stability and aromaticity. The introduction of metallocene can act as electron donators and carriers, leading to form continuous electron transfer channels and providing strong binding to metalloporphyrin in the CO_2RR process, thereby enhancing CO_2RR activity resulting from the participation of d-orbits in MCp_2 electron orbitals that enlarge the π-electron system of cyclopentadiene rings. Additionally, MOF-545 imparting with high porosity, large pore size (3.6 nm) and excellent chemical and thermal stability can serve as ideal platform to interact with MCp_2. When metallocene is implanted into the structure of MOFs, MCp_2 can serve as potential electron donator and carrier to enrich the electron density of MOF structure. Therefore, the FE_{CO} can get up to 97% at -0.7 V vs. RHE in the obtained MCp_2@MOF-545 composites (Figure 8), due to that the π-electron system of cyclopentadienyl ring might overlap with π-electron system of por-

DOI: 10.14102/j.cnki.0254-5861.2022-0075

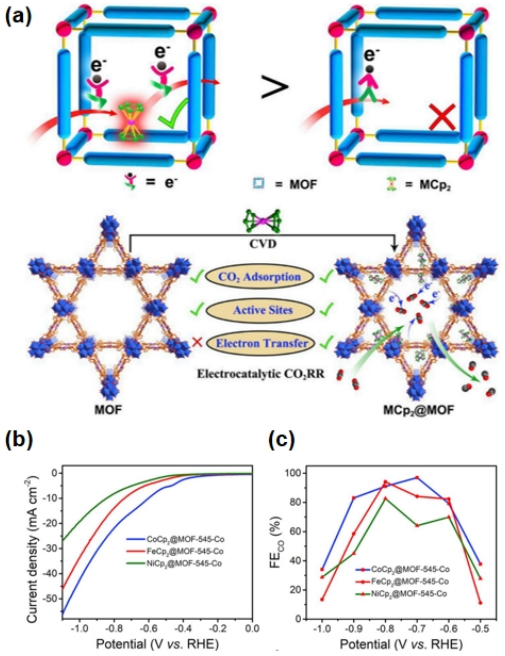

Figure 8. (a) The schematic presentation for MCp_2@MOF in electrocatalytic. (b) LSV curves of MCp_2@MOF in CO_2- and Ar-saturated 0.5 M $KHCO_3$. (c) FE_{CO} at different potentials. Reproduced with permission from Ref.[54]

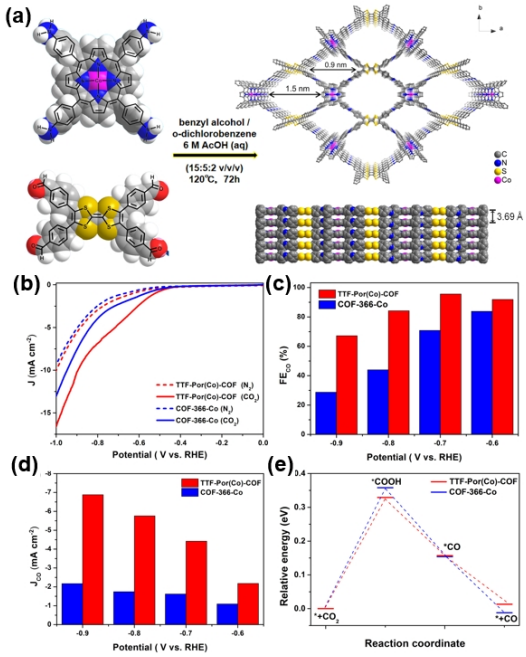

Figure 9. (a) Schematic illustration of the synthesis of two-dimensional TTF-Por(Co)-COF. (b) LSV curves in the N_2- and CO_2-saturated 0.5 M $KHCO_3$ electrolyte at a scan rate of 10 mV s^{-1}. (c) FE_{CO} from -0.6 to -0.9 V vs. RHE of TTF-Por(Co)-COF and COF-366-Co. (d) CO partial current density from -0.6 to -0.9 V vs. RHE of TTF-Por(Co)-COF and COF-366-Co. (e) Relative energy diagrams for CO_2 reduction reaction on TTF-Por(Co)-COF and COF-366-Co at 0 V vs. RHE. Reproduced with permission from Ref.[56]

phyrin. Besides, the strategy of embedding guest molecules into MOFs also would endow MOF-545 with higher CO_2 adsorption capability, larger amount of active sites and more favorable electron transfer property to largely enhance the electrocatalytic CO_2RR activity. The CO_2RR performance of conductive MOFs is compared in Table 1.

n CONDUCTIVE COFS CATALYSTS FOR CO_2RR

As mentioned above, most pristine COFs have relatively lower electrocatalytic activity due to their low electrical conductivity. In this part, we will introduce two mainly strategies: designing donor-acceptor heterojunction and fully π-conjugated COFs.

Donor-acceptor Heterojunction. By selecting linkers with their orient metal centers in a manner that allows for charge hopping or by incorporating redox-active linkages to construct donor-acceptor heterojunction is a good strategy to improve the conductivity of COFs. For instance, tetrathiafulvalene (TTF) as a kind of electron donors with high electron mobility is able to synthesize highly conductive charge-transfer crystals when constructed with electron acceptors.[55,56] Therefore, a well-defined TTF-based structure might have the potential for the particular alignment and stacking of TTF columns as conductive pathways.[57]

Recently, Huang and coworkers[58] construct a donor-acceptor (D-A) heterojunction in a porphyrin-based COF by integrating TTF strut (Figure 9a), in which highly efficient electronic transmission paths could be made to enhance electrocatalytic CO_2RR performance. Incorporating TTF units into frameworks not only can form π-π stacking columns, but also short S···S interactions can provide efficient charge-transport pathways. Besides, metalloporphyrin, possessing conjugated π-electron system, can act as excellent electron acceptor and electron transfer carrier. Combining TTF with metalloporphyrin can construct intermolecular charge-transfer pathway in a structure to largely enhance the electron transfer efficiency. Therefore, the electron conduction nature of TTF-Por(Co)-COF can reach 1.32 × 10^{-7} S m^{-1}, which is greater than that of COF-366-Co (6.5 × 10^{-9} S m^{-1}). Additionally, TTF-Por(Co)-COF has moderate CO_2 uptake capacities with 22 cm^3 g^{-1} at 298 K and 1 bar, which indicates the favorable CO_2 affinity for facilitating their electrocatalytic CO_2RR activity. Therefore, the current density of TTF-Por(Co)-COF can reach 6.88 mA cm^{-2} at the potential of -0.9 V vs. RHE, which is 3-fold to COF-366-Co (2.17 mA cm^{-2}).

As expected, TTF-Por(Co)-COF exhibits the best activity for **the** conversion of CO_2 to CO with high FE_{CO} of 95% at -0.7 V vs. RHE (Figure 9b, c, d and e). Thus, using TTF as linker unit to construct donor-acceptor heterojunction represents an efficient strategy to enhance its electron transfer capability of metal porphyrin-based COFs, which can construct efficient electron transmission pathway.

Furthermore, Huang and coworkers[59] continued to design a D-A heterojunction in a porphyrin-based COF by integrating thieno[3,2-b]thiophene-2,5-dicarbaldehyde (TT) into 2D TT-Por(Co)-COF (Figure 10a), in which the electron conduction value can get to 1.38 × 10^{-8} S m^{-1}. Moreover, after making TT-

DOI: 10.14102/j.cnki.0254-5861.2022-0075

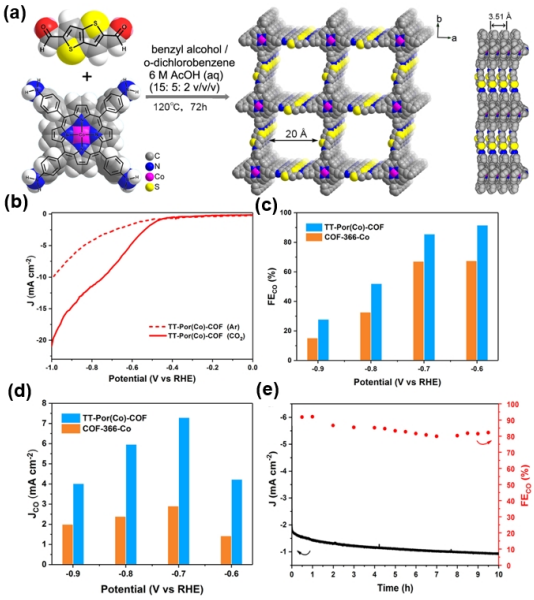

Figure 10. (a) Schematic synthesis of 2D TT-Por(Co)-COF. (b) LSV curves in CO_2- and Ar-saturated 0.5 M $KHCO_3$ at a scan rate of 10 mV s^{-1}. (c) FE_{CO} and (d) J_{co} from -0.6 to -0.9 V vs. RHE of TT-Por(Co)-COF and COF-366-Co. (e) Stability test of TT-Por(Co)-COF in CO_2-saturated 0.5 M $KHCO_3$ electrolyte at a potential of -0.6 V vs. RHE during 10 h. Reproduced with permission from Ref.[59]

Por(Co)-COF into nanosheets, they showed large partial current density of 7.28 mA cm^{-2} at -0.7 V vs. RHE, which is higher than COF-366-Co at the same potential, and the maximum FE_{CO} is high up to 91.4% at -0.6 V vs. RHE (Figure 10b, c and d). Besides, a long-term stability test of TT-Por(Co)-COF for 10 h proved its activity and stability (Figure 10e).

Clearly, the synergistic combination of TTF or TT and metalloporphyrin in these M-TTCOFs can serve as the role of gathering electron donating, electron migration, and electrocatalytic active components together in the electrocatalytic CO_2RR. And, TTF and TT with high electron mobility can construct efficient electron transmission pathway with metalloporphyrin. However, the relatively low current density and stability still limit its further application.

Fully π-conjugated COFs. The conductivity can be realized by using conjugated bonds to connect the catalytic sites and using tetragonal topology to create a fully π-conjugated network. Therefore, Huang and coworkers[60] synthesized a 2D conductive Ni-phthalocyanine-based COF (NiPc-COF) (Figure 11a) by constructing fully conjugated structure, in which the planar NiPc motifs were linked by the covalent pyrazine linkage. In these materials, metal phthalocyanines with M-N_4 structures have been considered as active sites for CO_2RR.[61-63] Notably, the covalent pyrazine linkage is critical as it endows the resulting framework with stability and conductivity. The CO_2 sorption isotherm measurement revealed that NiPc-COF has a high CO_2 adsorption capacity of 23 cm^3 g^{-1} at 298 K, proving its favorable CO_2 affinity, which is benefit for improving catalytic activity of CO_2RR. After making 2D COF into nanosheets, the robust conductive 2D NiPc-COF nanosheets exhibited large partial current density of 35 mA cm^{-2} at -1.1 V vs. RHE, and the maximum FE_{CO} can reach up to 99.1% at -0.9 V vs. RHE (Figure 11b and c). Moreover, the catalyst delivered a steady reduction current density for 10 h and the corresponding FE_{CO} was over 98%, suggesting good stability of the NiPc-COF catalyst (Figure 11d). Besides, the selectivity and current density of NiPc-COF nanosheets for the CO_2 to CO conversion compares favorably with the similar conductive COF electrocatalyst CoPc-PDQ-COF and exceeds most of the traditional COFs and MOFs (Figure 11e) due to the full in-plane π-delocalization for monolayers and ordered out-of-plane π-π stacking along the c axis. Overall, the excellent electrocatalytic performance of NiPc-COF for CO_2RR is attributed to a high conductivity of 3.77 × 10^{-6} S m^{-1}, which is several orders of magnitude higher than those of insulating COFs.

Recently, Huang and coworkers[64] also have constructed two catalysts with two types of sites, $CuPcF_8$-CoNPc-COF and $CuPcF_8$-CoPc-COF (Figure 12), which are constructed with the dioxin linkage. Although, the two COFs do not form full in-plane π-delocalization, the eclipsed stacking mode of metallophthalo-

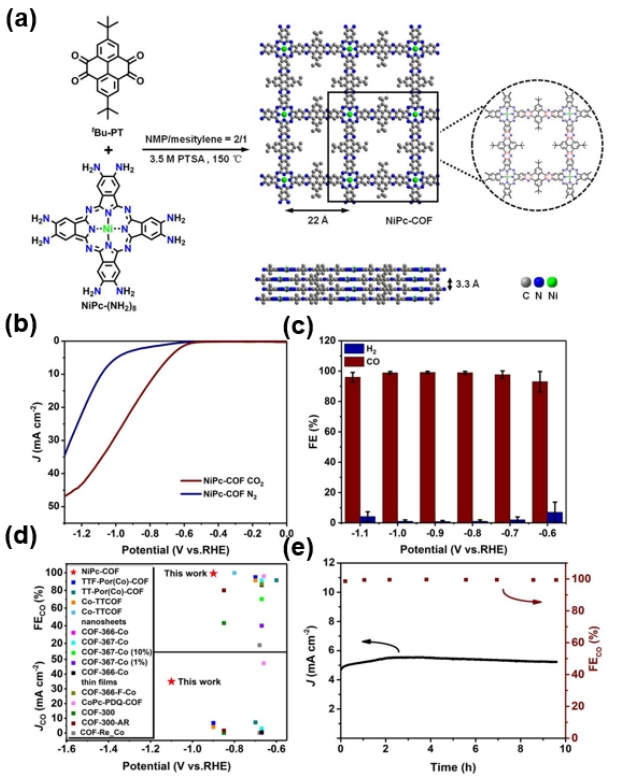

Figure 11. (a) Schematic illustration of the synthesis of two-dimensional NiPc-COF. (b) LSV curves of NiPc-COF in CO_2- and N_2-saturated 0.5 M $KHCO_3$ electrolyte at a scan rate of 10 mV S^{-1}. (c) FE_{CO} and FE_{H2} from -0.6 to -1.1 V vs. RHE of NiPc-COF in CO_2-saturated 0.5 M $KHCO_3$ electrolyte. (d) The comparison of the optimal FE_{CO} and CO partial current densities among the 2D conductive NiPc-COF and the reported COF electrocatalysts evaluated in a H-type electrochemical cell. (e) Stability test at -0.7 V vs. RHE for 10 h. Reproduced with permission from Ref.[60]

DOI: 10.14102/j.cnki.0254-5861.2022-0075

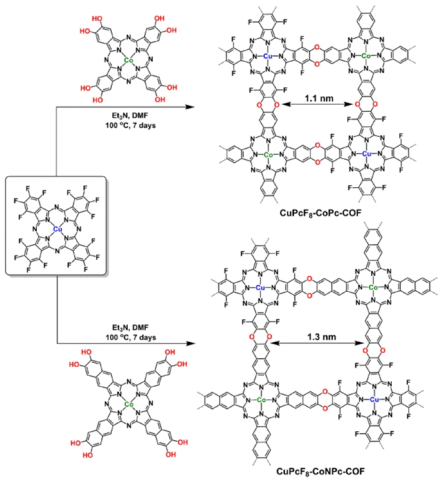

Figure 12. Schematic illustration synthesis of $CuPcF_8$-CoNPc-COF and $CuPcF_8$-CoPc-COF. Reproduced with permission from Ref.[64]

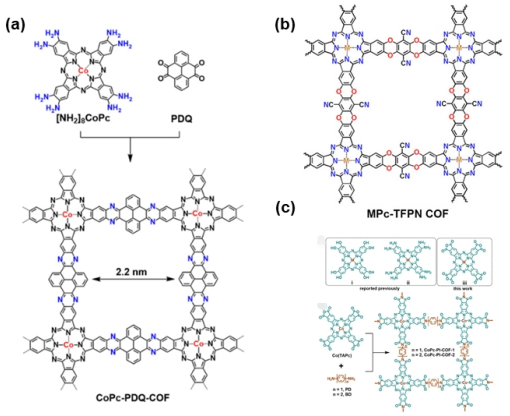

Figure 13. (a) Schematic illustration of the synthesis of two-dimensional CoPc-PDQ-COF. Reproduced with permission from Ref.[65] (b) Design and synthesis of MPc-TFPN COF. Reproduced with permission from Ref.[66] (c) Synthesis of CoPc-PI-COF-1 and CoPc-PI-COF-2. Reproduced with permission from Ref.[67]

cyanine units also supplies a high-speed pathway for electron transfer. However, the far apart catalytic sites and large pore diameter might prevent the tandem reaction. And, carbon monoxide is the main product for $CuPcF_8$-CoNPc-COF and $CuPcF_8$-CoPc-COF in CO_2RR, in which the maximum FE_{CO} can get up to 97%. Compared with $CuPcF_8$-CoPc-COF, $CuPcF_8$-CoNPc-COF has larger pore diameter, specific surface area and better CO_2 capacities, which is more benefit for improving catalytic activity of CO_2RR. Therefore, when tested in 0.5 M $CsHCO_3$, the TON values are as high as 108000 and 248000 for $CuPcF_8$CoPc-COF at -0.70 V and $CuPcF_8$-CoNPc-COF at -0.62 V in 24 h, respectively. Accordingly, their TOF values were calculated to be 1.25 and 2.87 s^{-1} under the same conditions.

In 2020, Jiang and coworkers[65] also constructed a catalytic CoPc-PDQ-COF for electrochemical CO_2RR (Figure 13a) in water, by exploring the robust phenazine linkage to connect metallophthalocyanine catalytic sites into a fully π-conjugated lattice. Besides, the stacking layer structure offers the conduction along the z direction across the π columns, so that electrons can directionally transport to catalytic sites over the shortest distance. The bulk conductivity of CoPc-PDQ-COF was calculated up to 3.68 × 10^{-3} S m^{-1} at 298 K by utilizing a four-point probe. Thus, the catalytic activity and efficiency will be enhanced as electrons from electrodes can be smoothly transported to the reaction center via the shortest pathway in a highly conductive and ordered network. Additionally, CoPc-PDQ-COF also exhibited long-term catalytic durability attributed to the stable fully π-conjugated structure. Overall, the increased conductivity would accelerate the electron transport efficiency during catalysis, decrease the Tafel slope, accelerate the rate determining step, and increase the TOF and TON. When tested at -0.66 V vs. RHE, the CoPc-PDQ-COF showed a large 49.4 mA cm^{-2} current density for effective conversion of CO_2 into CO with the FE_{CO} of 96%.

Additionally, Lan and coworkers[66] synthesized a series of dioxin-linked crystalline metallophthalocyanine COF (MPc-TFPN COF, M = Ni, Co, Zn) (Figure 13b), which can enhance their FE_{CO} by coupling with light. However, NiPc-TFPN COF has lower conductivity than NiPc-COF and CoPc-PDQ-COF due to the failure to form fully conjugated lattice. Although NiPc-TFPN COF exhibits excellent FE_{CO}, the low current density still limits its further applications.

As mentioned above, those conductive phthalocyanine-involved COFs have been constructed from the 2,3,9,10,16,17,23,24-octa-(hydroxyl/amino)-substituted phthalocyanine building blocks. In order to explore the excellent electrocatalytic CO_2RR properties of metallophthalocyanine compounds, Chen and coworkers[67] reported 2D conductive COFs CoPc-PI-COF-1 and CoPc-PI-COF-2 (Figure 13c) with a new kind of phthalocyanine building block, namely, tetraanhydrides of 2,3,9,10,16,17,23,24-octacarboxyphthalocyanine. These COFs also achieved highly electrical conductivity of 3.7 × 10^{-3} and 1.6 × 10^{-3} S m^{-1}, respectively, due to the full in-plane π-delocalization. Due to the same Co(II) electroactive sites together with similar permanent porosity and CO_2 adsorption capacity for CoPc-PI-COFs, the cathodes made up of COFs and carbon black displayed a similar FE_{CO} of 87-97% at applied potentials between -0.60 and -0.90 V vs. RHE in 0.5 M $KHCO_3$ solution. And, the TON of the CoPc-PI-COF-1 cathode is accumu-

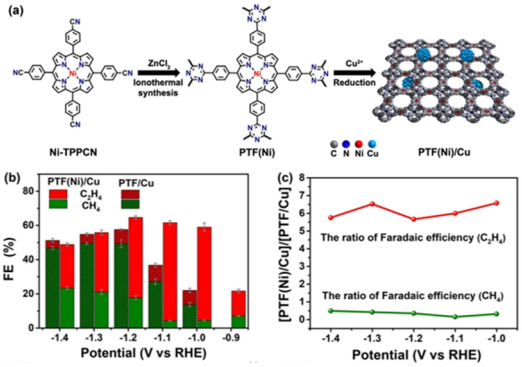

Figure 14. (a) Fabrication of PTF(Ni)/Cu with well dispersed copper sites from Ni-TPPCN. (b) FEs of C_2H_4 and CH_4 at different potentials on PTF(Ni)/Cu and PTF/Cu catalysts. (c) The FE ratio of PTF(Ni)/Cu to PTF/Cu. Reproduced with permission from Ref.[68]

DOI: 10.14102/j.cnki.0254-5861.2022-0075

Table 2. Comparison of the Highest Current Density, and Faraday Efficiency of Different Conductive COFs for CO_2RR

Catalysts	The highest J_{CO} (mA cm^{-2})	Electrolyte	The highest FE (%)	Conductivity (S m^{-1})	Ref.
TTF-Por(Co)-COF	6.88 (-0.9 V)	0.5 M $KHCO_3$	95 CO (-0.7 V)	1.32×10^{-7}	[58]
TT-Por(Co)-COF	7.28 (-0.7 V)	0.5 M $KHCO_3$	91.4 (-0.6 V)	1.38×10^{-8}	[59]
NiPc-COF	35 (-1.1 V)	0.5 M $KHCO_3$	99.1 (-0.9 V)	3.77×10^{-6}	[60]
CoPc-PDQ-COF	49.4 (-0.66 V)	0.5 M $KHCO_3$	96 CO (-0.66 V)	3.68×10^{-3}	[65]
CoPc-PI-COF-1	21.2 (-0.9 V)	0.5 M $KHCO_3$	99.8 CO (-0.8 V)	3.7×10^{-3}	[67]
CoPc-PI-COF-2	15.3 (-0.9 V)	0.5 M $KHCO_3$	97 CO (-0.8 V)	1.6×10^{-3}	[67]
PTF(Ni)/Cu	3.5 (-1.2 V)	0.1 M $KHCO_3$/0.1 M KCl	57.3 C_2H_4 (-1.1 V)	N.A.	[68]
$CuPcF_8$-CoPc-COF	15 (-0.62 V)	0.5 M $CsHCO_3$	91 CO (-0.7 V)	5.67×10^{-2}	[64]
$CuPcF_8$-CoNPc-COF	14.6 (-0.7 V)	0.5 M $CsHCO_3$	97 CO (-0.7 V)	2.14×10^{-1}	[64]

lated to 277000 with a TOF of 2.2 s^{-1} at -0.70 V after 40 h of continuous experiment.

Besides, to further expand the use of fully conjugated systems for CO_2RR, Huang et al. constructed a tandem catalyst PTF(Ni)/Cu by uniformly dispersing Cu NPs on PTF(Ni) containing the atomically isolated nickel-nitrogen sites for the CO_2 electroreduction reaction to significantly enhance the production of ethylene (Figure 14a).[68] The maximum FE_{C2H4} can reach up to 57.3% at -1.1 V vs. RHE, which is about 6 times higher than that of the non-tandem contrast catalyst PTF/Cu (Figure 13b and c).

Clearly, the high conductivity of those COFs originates from the fully π-conjugated yet stacked structure that allows electron transport over the whole skeleton. In addition, the catalytic efficiency will be enhanced when electrons from electrodes can be smoothly transported to the reaction center via the shortest pathway for electrocatalytic CO_2RR. The CO_2RR performance of conductive COFs is compared in Table 2.

n CONCLUSION

Compared to traditional catalytic materials, MOFs and COFs have emerged as a new sub-field in electrocatalysis due to their high specific surface areas and porous structures that provide more exposed active sites and facile mass transport pathways. Meanwhile, specific products in the electrocatalytic CO_2RR can be generated by tuning their electronic and geometric features at the atomic/molecular level. Especially, molecular catalysts possess well-defined structures of active sites that enable mechanistic studies to address the structure-mechanism-activity relationship. Despite the enormous potential of traditional MOF and COF materials for electrocatalysis CO_2RR, the problem of poor electrical conductivity severely limits their further applications. Therefore, the design and construction of MOF and COF materials with excellent electrical conductivity are the key for their further development. To give younger researchers a clearer understanding of the differences between conductive and non-conductive MOFs and COFs, we summarize the characteristics of conductive MOFs and COFs as follows: (1) Metals and ligand moieties with well-matched energy levels and good orbital overlap can result in small band gaps and high charge mobilities, both of which are favorable for conductivity. Therefore, MOFs and COFs with oxygen or nitrogen coordinating to the metals usually have better electrical conductivity, in which the energy matching and metal-ligand orbital overlap are improved. (2) For the majority of 2D MOFs and COFs, charge transport within the π-d conjugated planes has been invoked to be the dominant mechanism behind conductivity. Meanwhile, the π-π interlayer interactions in the bulk structures of MOFs and COFs may also be important for contributing to charge delocalization. (3) MOFs and COFs can be introduced containing redox active groups and active guest molecules to induce conductivity.

In addition to the above strategies, MOF and COF-derived materials have also attracted numerous attention for they to some extent inherit advantages of their parent materials and provide enhanced conductivity and stability via facile calcination-thermolysis strategies.[69-76] However, the pyrolysis process may cause undesirable structural changes and even destroy finer framework structures, resulting in the mechanism of the electrocatalytic process uncertain. To overcome this challenge while retaining the capabilities to atomically precisely control the structure, well-defined MOFs and COFs also can be composited with conductive supporting materials (e.g., CPs, graphene, and carbon nanotubes) that provide adequate conducting channels and more effective surface area for forming MOF/COF-based hybrid systems. Besides, it is also a good strategy to apply MOF and COF materials for the photocatalytic reduction of CO_2.[77-81]

In this review, we mainly introduced several design strategies for conductive MOFs and COFs for electrocatalytic CO_2RR. Additionally, we summarized the advances of conductive MOFs and COFs catalysts in CO_2RR and compared with traditional MOFs and COFs catalysts. Conductive MOFs and COFs materials have exhibited great potentials in catalyzing CO_2RR due to their higher current density than traditional materials. Granted, deliberate design for improving conductivity of framework-based materials might pave the way for fabricating excellent CO_2RR catalysts in laboratories, but exploring large-scale synthetic methods with high yields and affordable cost is required for industrial applications. For industrial application, the current density should be higher than 300 mA cm^{-2}, FE higher than 80%, cell voltage less than 1.8 V and stability over 80000 hours to make CO economically viable.[82-84] Therefore, the challenges are still in need on the following aspects.

Firstly, although conductive MOFs and COFs have achieved great progress in the electrocatalytic CO_2 reduction reactions, the current density cannot meet the industrial requirements. Therefore, developing conductive MOFs and COFs with better conductivity will create new opportunities to design highly efficient

DOI: 10.14102/j.cnki.0254-5861.2022-0075

electrocatalysts. Besides, most of the conductive MOFs and COFs only produce CO, while multi-electron transfer products such as ethylene and ethanol are much more desirable. Additionally, it still needs to improve the conductive MOFs and COFs in strong alkalinity and acidity aqueous electrolytes. Finally, the fabrication cost-effective of MOF and COF materials needs to enable their application on a large scale.

In summary, as effective electrocatalysts for CO_2RR, MOF and COF materials should further improve the electrical conductivity and stability. Looking forward, using conductive MOFs and COFs as substrates to anchor catalytic sites and then to synergistically electrocatalyze for CO_2RR is also a good strategy to improve current density and selectivity..

n ACKNOWLEDGEMENTS

The work was supported by the National Key Research and Development Program of China (Nos. 2018YFA0208600, 2018YFA0704502), NSFC (Nos. 21871263, 22071245, 22033008), and Fujian Science & Technology Innovation Laboratory for Optoelectronic Information of China (No. 2021ZZ103).

n AUTHOR INFORMATION

Corresponding authors. Emails: ybhuang@fjirsm.ac.cn and rcao@fjirsm.ac.cn

n ADDITIONAL INFORMATION

Full paper can be accessed via
http://manu30.magtech.com.cn/jghx/EN/10.14102/j.cnki.0254-5861.2022-0075
For submission: https://mc03.manuscriptcentral.com/cjsc

n REFERENCES

(1) Drechsler, M.; Egerer, J.; Lange, M.; Masurowski, F.; Meyerho, J.; Oehlmann, M. Efficient and equitable spatial allocation of renewable power plants at the country scale. *Nat. Energy* **2017**, 2, 17124.

(2) Leitner, W.; Quadrelli, E. A.; Schloegl, R. Harvesting renewable energy with chemistry. *Green Chem.* **2017**, 19, 2307-2308.

(3) Siria, A.; Bocquet, M. L.; Bocquet, L. New avenues for the large-scale harvesting of blue energy. *Nat. Rev. Chem.* **2017**, 1, 0091.

(4) Marttunen, M.; Belton, V.; Lienert, J. Are objectives hierarchy related biases observed in practice? A meta-analysis of environmental and energy applications of Multi-Criteria Decision Analysis. *Eur. J. Oper. Res.* **2018**, 265, 178-194.

(5) Liu, S. H.; Li, Y.; Ding, K. N.; Chen, W. K.; Zhang, Y. F.; Lin, W. Mechanism on carbon vacancies in polymeric carbon nitride for CO_2 photoreduction. *Chin. J. Struct. Chem*. **2020**, 39, 2068-2076.

(6) Li, Z.; Zhai, L.; Ge, Y.; Huang, Z.; Shi, Z.; Liu, J.; Zhai, W.; Liang, J.; Zhang, H. Wet-chemical synthesis of two-dimensional metal nanomaterials for electrocatalysis. *Natl. Sci. Rev*. **2021**, DOI: 10.1093/nsr/nwab142.

(7) Zhou, Y. G.; Kang, Y.; Huang, J. Fluidized electrocatalysis. *CCS Chem.* **2020**, *2*, 31-41.

(8) Li, G. W.; Yang, Q.; Manna, K.; Mu, Q. G.; Fu, C. G.; Sun, Y.; Felse, C. Magnetocatalysis: the interplay between the magnetic field and electrocatalysis. *CCS Chem.* **2021**, 3, 2259-2267.

(9) Yang, D.; Zhu, Q.; Chen, C.; Liu, H.; Liu, Z.; Zhao, Z.; Zhang, X.; Liu, S.; Han, B. Selective electroreduction of carbon dioxide to methanol on copper selenide nanocatalysts. *Nat. Commun.* **2019**, 10, 677.

(10) Zhang, M. D.; Yi, J. D.; Huang, Y. B.; Cao, R. Covalent triazine frameworks-derived N,P dual-doped porous carbons for highly efficient electrochemical reduction of CO_2. *Chin. J. Struct. Chem*. **2021**, 40, 1213-1222.

(11) Zhang, W.; Hu, Y.; Ma, L.; Zhu, G.; Wang, Y.; Xue, X.; Chen, R.; Yang, S.; Jin, Z. Progress and perspective of electrocatalytic CO_2 reduction for renewable carbonaceous fuels and chemicals. *Adv. Sci.* **2018**, 5.

(12) Hou, S. S.; Xu, Z. T.; Zhang, Y. K.; Xie, K.; Gan, L. Z. Enhanced CO_2 electrolysis with Mn-doped $SrFeO_3$-delta cathode. *Chin. J. Struct. Chem*. **2020**, 39, 1662-1668.

(13) Ye, K.; Wang, G. X.; Bao, X. H. Electrodeposited Sn-based catalysts for CO_2 electroreduction. *Chin. J. Struct. Chem*. **2020**, 39, 206-213.

(14) Yang, D.; Sun, Y. N; Cai, X.; Hu, W. G.; Dai, Y. H.; Zhu, Y.; Yang, Y. H. Catalytic conversion of C1 molecules on atomically precise metal nanoclusters. *CCS Chem.* **2021**, 4, 66-94.

(15) Xu, Z. T.; Xie, K. Enhanced CO_2 electrolysis with metal-oxide interface structures. *Chin. J. Struct. Chem*. **2021**, 40, 31-41.

(16) Peterson, A. A.; Norskov, J. K. Activity descriptors for CO_2 electroreduction to methane on transition-metal catalysts. *J. Phys. Chem. Lett.* **2012**, 3, 251-258.

(17) Klingan, K.; Kottakkat, T.; Jovanov, Z. P.; Jiang, S.; Pasquini, C.; Scholten, F.; Kubella, P.; Bergmann, A.; Roldan Cuenya, B.; Roth, C.; Dau, H. Reactivity determinants in electrodeposited Cu foams for electrochemical CO_2 reduction. *ChemSusChem* **2018**, 11, 3449-3459.

(18) Corbin, N.; Zeng, J.; Williams, K.; Manthiram, K. Heterogeneous molecular catalysts for electrocatalytic CO_2 reduction. *Nano Res.* **2019**, 12, 2093-2125.

(19) Feng, D. M.; Zhu, Y. P.; Chen, P.; Ma, T. Y. Recent advances in transition-metal-mediated electrocatalytic CO_2 reduction: from homogeneous to heterogeneous systems. *Catalysts* **2017**, 7, 373.

(20) Fukuzumi, S.; Lee, Y. M.; Ahn, H. S.; Nam, W. Mechanisms of catalytic reduction of CO_2 with heme and nonheme metal complexes. *Chem. Sci.* **2018**, 9, 6017-6034.

(21) Wang, N.; Feng, L.; Shang, Y.; Zhao, J.; Cai, Q.; Jin, P. Two-dimensional iron-tetracyanoquinodimethane (Fe-TCNQ) monolayer: an efficient electrocatalyst for the oxygen reduction reaction. *RSC Adv.* **2016**, 6, 72952-72958.

(22) He, C.; Liang, J.; Zou, Y. H.; Yi, J. D.; Huang, Y. B.; Cao, R. Metal-organic frameworks bonded with metal N-heterocyclic carbenes for efficient catalysis. *Natl. Sci. Rev.* **2021**, DOI: 10.1093/nsr/nwab157.

(23) Zheng, S.; Li, Q.; Xue, H.; Pang, H.; Xu, Q. A highly alkaline-stable metal oxide@metal-organic framework composite for high-performance electrochemical energy storage. *Natl. Sci. Rev.* **2020**, 7, 305-314.

(24) Cui, P. P.; Liu, Y.; Zhai, H. G.; Zhu, J. P.; Yan, W. N.; Yang, Y. M. Two copper-organic frameworks constructed from the flexible dicarboxylic ligands. *Chin. J. Struct. Chem.* **2020**, 39, 368-374.

(25) Liang, Z.; Wang, H. Y.; Zheng, H.; Zhang, W.; Cao, R. Porphyrin-based frameworks for oxygen electrocatalysis and catalytic reduction of carbon dioxide. *Chem. Soc. Rev.* **2021**, 50, 2540-2581.

(26) Wang, Y.; Zhang, X. P.; Lei, H.; Guo, K.; Xu, G.; Xie, L.; Li, X.; Zhang, W.; Apfel, U. P.; Cao, R. Tuning electronic structures of covalent Co porphyrin polymers for electrocatalytic CO_2 reduction in aqueous solutions. *CCS Chem.* **2022**, DOI: 10.31635/ccschem.022.202101706.

(27) Wu, X. M.; Liu, M. M.; Guo, H. X.; Ying, S. M.; Chen, Z. X. Polyoxovanadate-based MOFs microsphere constructed from 3-D discrete

nano-sheets as supercapacitor. *Chin. J. Struct. Chem.* **2021**, 40, 994-998.
(28) Liang, Y.; Xu, X. D.; Ni, J. L.; Li, J. F.; Wang, F. M. Synthesis, structure and fluorescence property of new Cd-MOFs based on a tetraphenylethylene (tpe) ligand. *Chin. J. Struct. Chem.* **2021**, 40, 193-198.
(29) Zhang, X.; Chen, Z. X.; Yang, Y. T.; Deng, M. L.; Weng, L. H. Effect of fluorination on the crystal structure, stability and gas adsorption property in zinc(II) metal-organic frameworks. *Chin. J. Struct. Chem.* **2022**, 41, 2202049-2202056.
(30) Hinogami, R.; Yotsuhashi, S.; Deguchi, M.; Zenitani, Y.; Hashiba, H.; Yamada, Y. Electrochemical reduction of carbon dioxide using a copper rubeanate metal organic framework. *ECS Electrochem. Lett.* **2012**, 1, H17-H19
(31) Hod, I.; Sampson, M. D.; Deria, P.; Kubiak, C. P.; Farha, O. K.; Hupp, J. T. Fe-porphyrin-based metal-organic framework films as high-surface concentration, heterogeneous catalysts for electrochemical reduction of CO_2. *ACS Catal.* **2015**, 5, 6302-6309.
(32) Kornienko, N.; Zhao, Y.; Kley, C. S.; Zhu, C.; Kim, D.; Lin, S.; Chang, C. J.; Yaghi, O. M.; Yang, P. Metal-organic frameworks for electrocatalytic reduction of carbon dioxide. *J. Am. Chem. Soc.* **2015**, 137, 14129-14135.
(33) Jiang, X.; Li, H.; Xiao, J.; Gao, D.; Si, R.; Yang, F.; Li, Y.; Wang, G.; Bao, X. Carbon dioxide electroreduction over imidazolate ligands coordinated with Zn(II) center in ZIFs. *Nano Energy* **2018**, 52, 345-350.
(34) Wang, Y.; Hou, P.; Wang, Z.; Kang, P. Zinc imidazolate metal-organic frameworks (ZIF-8) for electrochemical reduction of CO_2 to CO. *ChemPhysChem* **2017**, 18, 3142-3147.
(35) Yang, Z.; Zhang, X.; Long, C.; Yan, S.; Shi, Y.; Han, J.; Zhang, J.; An, P.; Chang, L.; Tang, Z. Covalently anchoring cobalt phthalocyanine on zeolitic imidazolate frameworks for efficient carbon dioxide electroreduction. *CrystEngComm* **2020**, 22, 1619-1624.
(36) Yang, X.; Li, Q. X.; Chi, S. Y.; Li, H. F.; Huang, Y. B.; Cao, R. Hydrophobic perfluoroalkane modified metal-organic frameworks for the enhanced electrocatalytic reduction of CO. *SmartMat* **2022**, 3, 163-172.
(37) Lin, S.; Diercks, C. S.; Zhang, Y. B.; Kornienko, N.; Nichols, E. M.; Zhao, Y.; Paris, A. R.; Kim, D.; Yang, P.; Yaghi, O. M.; Chang, C. J. Covalent organic frameworks comprising cobalt porphyrins for catalytic CO_2 reduction in water. *Science* **2015**, 349, 1208-1213.
(38) Cheung, P. L.; Lee, S. K.; Kubiak, C. P. Facile solvent-free synthesis of thin iron porphyrin COFs on carbon cloth electrodes for CO_2 reduction. *Chem. Mater.* **2019**, 31, 1908-1919.
(39) Chi, S. Y.; Chen, Q.; Zhao, S. S.; Si, D. H.; Wu, Q. J.; Huang, Y. B.; Cao, R. Three-dimensional porphyrinic covalent organic frameworks for highly efficient electroreduction of carbon dioxide. *J. Mater. Chem. A* **2022**, 10, 4653-4659.
(40) Diercks, C. S.; Lin, S.; Komienko, N.; Kapustin, E. A.; Nichols, E. M.; Zhu, C.; Zhao, Y.; Chang, C. J.; Yaghi, O. M. Reticular electronic tuning of porphyrin active sites in covalent organic frameworks for electrocatalytic carbon dioxide reduction. *J. Am. Chem. Soc.* **2018**, 140, 1116-1122.
(41) Popov, D. A.; Luna, J. M.; Orchanian, N. M.; Haiges, R.; Downes, C. A.; Marinescu, S. C. A 2,2'-bipyridine-containing covalent organic framework bearing rhenium(I) tricarbonyl moieties for CO_2 reduction. *Dalton Trans* **2018**, 47, 17450-17460.
(42) Yi, J. D.; Si, D. H.; Xie, R.; Yin, Q.; Zhang, M. D.; Wu, Q.; Chai, G. L.; Huang, Y. B.; Cao, R. Conductive two-dimensional phthalocyanine-based metal-organic framework nanosheets for efficient electroreduction of CO_2. *Angew. Chem. Int. Ed.* **2021**, 60, 17108.
(43) Zhang, M. D.; Si, D. H.; Yi, J. D.; Yin, Q.; Huang, Y. B.; Cao, R. Conductive phthalocyanine-based metal-organic framework as a highly efficient electrocatalyst for carbon dioxide reduction reaction. *Sci. China Chem.* **2021**, 64, 1332-1339.
(44) Meng, Z.; Luo, J.; Li, W.; Mirica, K. A. Hierarchical tuning of the performance of electrochemical carbon dioxide reduction using conductive two-dimensional metallophthalocyanine based metal-organic frameworks. *J. Am. Chem. Soc.* **2020**, 142, 21656-21669.
(45) Zhong, H.; Ghorbani-Asl, M.; Ly, K. H.; Zhang, J.; Ge, J.; Wang, M.; Liao, Z.; Makarov, D.; Zschech, E.; Brunner, E.; Weidinger, I. M.; Zhang, J.; Krasheninnikov, A. V.; Kaskel, S.; Dong, R.; Feng, X. Synergistic electroreduction of carbon dioxide to carbon monoxide on bimetallic layered conjugated metal-organic frameworks. *Nat. Commun.* **2020**, 11, 1409.
(46) Qiu, X. F.; Zhu, H. L.; Huang, J. R.; Liao, P. Q.; Chen, X. M. Highly selective CO_2 electroreduction to C_2H_4 using a metal-organic framework with dual active sites. *J. Am. Chem. Soc.* **2021**, 143, 7242-7246.
(47) Yi, J. D.; Si, D. H.; Xie, R.; Yin, Q.; Zhang, M. D.; Wu, Q.; Chai, G. L.; Huang, Y. B.; Cao, R. Conductive two-dimensional phthalocyanine-based metal-organic framework nanosheets for efficient electroreduction of CO_2. *Angew. Chem. Int. Ed.* **2021**, 60, 17108.
(48) Manthiram, K.; Beberwyck, B. J.; Alivisatos, A. P. Enhanced electrochemical methanation of carbon dioxide with a dispersible nanoscale copper catalyst. *J. Am. Chem. Soc.* **2014**, 136, 13319-13325.
(49) Karapinar, D.; Huan, N. T.; Ranjbar Sahraie, N.; Li, J.; Wakerley, D.; Touati, N.; Zanna, S.; Taverna, D.; Galvão Tizei, L. H.; Zitolo, A.; Jaouen, F.; Mougel, V.; Fontecave, M. Electroreduction of CO_2 on single-site copper-nitrogen-doped carbon material: selective formation of ethanol and reversible restructuration of the metal sites. *Angew. Chem. Int. Ed.* **2019**, 58, 15098-15103.
(50) Yang, H.; Wu, Y.; Li, G.; Lin, Q.; Hu, Q.; Zhang, Q.; Liu, J.; He, C. Scalable production of efficient single-atom copper decorated carbon membranes for CO_2 electroreduction to methanol. *J. Am. Chem. Soc.* **2019**, 141, 12717-12723.
(51) Kibria, M. G.; Edwards, J. P.; Gabardo, C. M.; Dinh, C. T.; Seifitokaldani, A.; Sinton, D.; Sargent, E. H. Electrochemical CO_2 reduction into chemical feedstocks: from mechanistic electrocatalysis models to system design. *Adv. Mater.* **2019**, 31, 1807166.
(52) Wang, Y. R.; Huang, Q.; He, C. T.; Chen, Y.; Liu, J.; Shen, F. C.; Lan, Y. Q. Oriented electron transmission in polyoxometalate-metalloporphyrin organic framework for highly selective electroreduction of CO_2. *Nat. Commun.* **2018**, 9, 4466.
(53) Hod, I.; Sampson, M. D.; Deria, P.; Kubiak, C. P.; Farha, O. K.; Hupp, J. T. Fe-Porphyrin-based metal-organic framework films as high-surface concentration, heterogeneous catalysts for electrochemical reduction of CO_2. *ACS Catal.* **2015**, 5, 6302-6309.
(54) Xin, Z.; Wang, Y. R.; Chen, Y.; Li, W. L.; Dong, L. Z.; Lan, Y. Q. Metallocene implanted metalloporphyrin organic framework for highly selective CO_2 electroreduction. *Nano Energy* **2020**, 67, 104233.
(55) Narayan, T. C.; Miyakai, T.; Seki, S.; Dincă, M. High charge mobility in a tetrathiafulvalene-based microporous metal-organic framework. *J. Am. Chem. Soc.* **2012**, 134, 12932-12935.
(56) Jana, A.; Bahring, S.; Ishida, M.; Goeb, S.; Canevet, D.; Salle, M.; Jeppesen, J. O.; Sessler, J. L. Functionalised tetrathiafulvalene-(TTF-) macrocycles: recent trends in applied supramolecular chemistry. *Chem. Soc. Rev.* **2018**, 47, 5614-5645.
(57) Dong, W. l.; Wang, L.; Ding, H. M.; Zhao, L.; Wang, D.; Wang, C.; Wan, L. J. Substrate orientation effect in the on-surface synthesis of

DOI: 10.14102/j.cnki.0254-5861.2022-0075

tetrathiafulvalene-integrated single-layer covalent organic frameworks. *Langmuir* **2015**, 31, 11755-11759.
(58) Wu, Q.; Xie, R. K.; Mao, M. J.; Chai, G.; Yi, J. D.; Zhao, S. S.; Huang, Y. B.; Cao, R. Integration of strong electron transporter tetrathiafulvalene into metalloporphyrin-based covalent organic framework for highly efficient electroreduction of CO_2. *ACS Energy Lett.* **2020**, 5, 1005-1012.
(59) Wu, Q.; Mao, M. J.; Wu, Q. J.; Liang, J.; Huang, Y. B.; Cao, R. Construction of donor-acceptor heterojunctions in covalent organic framework for enhanced CO_2 electroreduction. *Small* **2021**, 17, 2004933.
(60) Zhang, M. D.; Si, D. H.; Yi, J. D.; Zhao, S. S.; Huang, Y. B.; Cao, R. Conductive phthalocyanine-based covalent organic framework for highly efficient electroreduction of carbon dioxide. *Small* **2020**, 16, 2005254.
(61) Zhang, X.; Wu, Z.; Zhang, X.; Li, L.; Li, Y.; Xu, H.; Li, X.; Yu, X.; Zhang, Z.; Liang, Y.; Wang, H. Highly selective and active CO_2 reduction electrocatalysts based on cobalt phthalocyanine/carbon nanotube hybrid structures. *Nat. Commun.* **2017**, 8, 14675.
(62) Wu, H.; Zeng, M.; Zhu, X.; Tian, C.; Mei, B.; Song, Y.; Du, X. L.; Jiang, Z.; He, L.; Xia, C.; Dai, S. Defect engineering in polymeric cobalt phthalocyanine networks for enhanced electrochemical CO_2 reduction. *ChemElectroChem* **2018**, 5, 2717.
(63) Morlanes, N.; Takanabe, K.; Rodionov, V. Simultaneous reduction of CO_2 and splitting of H_2O by a single immobilized cobalt phthalocyanine electrocatalyst. *ACS Catal.* **2016**, 6, 3092-3095.
(64) Yue, Y.; Cai, P.; Xu, K.; Li, H.; Chen, H.; Zhou, H. C.; Huang, N. Stable bimetallic polyphthalocyanine covalent organic frameworks as superior electrocatalysts. *J. Am. Chem. Soc.* **2021**, 143, 18052-18060.
(65) Huang, N.; Lee, K. H.; Yue, Y.; Xu, X.; Irle, S.; Jiang, Q.; Jiang, D. A stable and conductive metallophthalocyanine framework for electrocatalytic carbon dioxide reduction in water. *Angew. Chem. Int. Ed.* **2020**, 59, 16587-16593.
(66) Lu, M.; Zhang, M.; Liu, C. G.; Liu, J.; Shang, L. J.; Wang, M.; Chang, J. N.; Li, S. L.; Lan, Y. Q. Stable dioxin-linked metallophthalocyanine covalent organic frameworks (COFs) as photo-coupled electrocatalysts for CO_2 reduction. *Angew. Chem. Int. Ed.* **2020**, 59, 23641-23648.
(67) Han, B.; Ding, X.; Yu, B. Q.; Wu, H.; Zhou, W.; Liu, W. P.; Wei, C. Y.; Chen, B. T.; Qi, D. D.; Wang, H. L.; Wang, K.; Chen, Y. L.; Chen, B. L.; Jiang, J. Z. Two-dimensional covalent organic frameworks with cobalt(II)-phthalocyanine sites for efficient electrocatalytic carbon dioxide reduction. *J. Am. Chem. Soc.* **2021**, 7104-7113.
(68) Meng, D. L.; Zhang, M. D.; Si, D. H.; Mao, M. J.; Hou, Y.; Huang, Y. B.; Cao, R. Highly selective tandem electroreduction of CO_2 to ethylene over atomically isolated nickel-nitrogen site/copper nanoparticle catalysts. *Angew. Chem. Int. Ed.* **2021**, 60, 25485-25492.
(69) Li, P.; Zeng, H. C. Advanced oxygen evolution catalysis by bimetallic Ni-Fe phosphide nanoparticles encapsulated in nitrogen, phosphorus, and sulphur tri-doped porous carbon. *Chem. Commun.* **2017**, 53, 6025-6028.
(70) Zhang, H.; Liu, X.; Wu, Y.; Guan, C.; Cheetham, A. K.; Wang, J. MOF-derived nanohybrids for electrocatalysis and energy storage: current status and perspectives. *Chem. Commun.* **2018**, 54, 5268-5288.
(71) Yilmaz, G.; Yam, K. M.; Zhang, C.; Fan, H. J.; Ho, G. W. In situ transformation of MOFs into layered double hydroxide embedded metal sulfides for improved electrocatalytic and supercapacitive performance. *Adv. Mater.* **2017**, 29, 1606814.
(72) Jiang, Y.; Liu, H.; Tan, X.; Guo, L.; Zhang, J.; Liu, S.; Guo, Y.; Zhang, J.; Wang, H.; Chu, W. Monoclinic ZIF-8 nanosheet-derived 2D carbon nanosheets as sulfur immobilizer for high-performance lithium sulfur batteries. *ACS Appl. Mater. Interfaces* **2017**, 925239-25249.
(73) Li, W.; Hu, S.; Luo, X.; Li, Z.; Sun, X.; Li, M.; Liu, F.; Yu, Y. Confined amorphous red phosphorus in MOF-derived N-doped microporous carbon as a superior anode for sodium-ion battery. *Adv. Mater.* **2017**, 29, 1605820.
(74) Jiao, L.; Zhu, J.; Zhang, Y.; Yang, W.; Zhou, S.; Li, A.; Xie, C.; Zheng, X.; Zhou, W.; Yu, S. H.; Jiang, H. L. Non-bonding interaction of neighboring Fe and Ni single-atom pairs on MOF-derived N-doped carbon for enhanced CO_2 electroreduction. *J. Am. Chem. Soc.* **2021**, 143, 19417-19424.
(75) Zhang, Y.; Jiao, L.; Yang, W.; Xie, C.; Jiang, H. L. Rational fabrication of low-coordinate single-atom Ni electrocatalysts by MOFs for highly selective CO_2 reduction. *Angew. Chem. Int. Ed.* **2021**, 60, 7607-7611.
(76) Gong, Y. N.; Jiao, L.; Qian, Y.; Pan, C. Y.; Zheng, L.; Cai, X.; Liu, B.; Yu, S. H.; Jiang, H. L. Regulating the coordination environment of MOF-templated single-atom nickel electrocatalysts for boosting CO_2 reduction. *Angew. Chem. Int. Ed.* **2020**, 59, 2705-2709.
(77) Zou, L.; Sa, R.; Zhong, H.; Lv, H.; Wang, X.; Wang, R. Photoelectron transfer mediated by the interfacial electron effects for boosting visible-light-driven CO_2 reduction. *ACS Catal.* **2022**, 12, 3550-3557.
(78) Lin, H. X.; Chen, C. P.; Zhou, T. H.; Zhang, J. Two-dimensional covalent-organic frameworks for photocatalysis: the critical roles of building block and linkage. *Sol. RRL* **2021**, 5, 2000458.
(79) Lin, H.; Xu, Y.; Wang, B.; Li, D. S.; Zhou, T.; Zhang, J. Postsynthetic modification of metal-organic frameworks for photocatalytic applications. *Small Struct.* **2022**, DOI: 10.1002/sstr.202100176.
(80) Pan, Y. T.; Qian, Y. Y.; Zheng, X. S.; Chu, S. Q.; Yang, Y. J.; Ding, C. M.; Wang, X.; Yu, S. H.; Jiang, H. L. Precise fabrication of single-atom alloy co-catalyst with optimal charge state for enhanced photocatalysis. *Natl. Sci. Rev.* **2020**, 8, nwaa224.
(81) Liu, S. H.; Li, Y.; Ding, K. N.; Chen, W. K.; Zhang, Y. F.; Lin, W. Mechanism on carbon vacancies in polymeric carbon nitride for CO_2 photoreduction. *Chin. J. Struct. Chem*. **2020**, 39, 2068-2076.
(82) Kibria, M. G.; Edwards, J. P.; Gabardo, C. M.; Dinh, C. T.; Seifitokaldani, A.; Sinton, D.; Sargent, E. H. Electrochemical CO_2 reduction into chemical feedstocks: from mechanistic electrocatalysis models to system design. *Adv. Mater.* **2019**, 31, 1807166.
(83) Ni, Y.; Miao, L.; Wang, J.; Liu, J.; Yuan, M.; Chen, J. Pore size effect of graphyne supports on CO_2 electrocatalytic activity of Cu single atoms. *Chem. Phys.* **2020**, 22, 1181-1186.
(84) Gao, F. Y.; Bao, R. C.; Gao, M. R.; Yu, S. H. Electrochemical CO_2-to-CO conversion: electrocatalysts, electrolytes, and electrolyzers. *J. Mater. Chem. A* **2020**, 8, 15458-15478.

Received: April 3, 2022
Accepted: April 29, 2022
Published: May 20, 2022

Chang-Pu Wan obtained his BE degree from the Qingdao University in 2020. Currently, he studies as a master student in Prof. Rong Cao's group in the Fujian Institute of Research on the Structure of Matter (FJIRSM), CAS. His research focuses on porous frameworks materials (MOFs, COFs) for CO_2 heterogeneous catalysis.

Jun-Dong Yi received his bachelor's degree from the School of Materials Science and Engineering, Central South University in 2013. Then he received his PhD degree in Fujian Institute of Research on the Structure of Matter (FJIRSM), Chinese Academy of Sciences in 2018. His current research interest focuses on carbon dioxide cycle system, including carbon dioxide enrichment, carbon dioxide electrolysis, and the improvement of carbon dioxide electrolysis device.

Yuan-Biao Huang obtained his PhD (2009) under the supervision of Prof. Guo-Xin Jin from Fudan University. In the same year, he joined Prof. Rong Cao's group at FJIRSM, CAS. In 2014, he joined Prof. Qiang Xu's group at AIST (National Institute of Advanced Industrial Science and Technology) as a JSPS (Japan Society for the Promotion of Science) invited fellow. In 2015, he moved back to FJIRSM, CAS and since 2017, he has been a professor at FJIRSM. His research interests include porous ionic frameworks and conducting materials (MOFs, COFs) for CO_2-involved heterogeneous catalysis.

Rong Cao received his bachelor's degree from University of Science and Technology of China in 1986 and obtained his PhD (1993) in FJIRSM (Fujian Institute of Research on the Structure of Matter), Chinese Academy of Sciences. Following post-doctoral experience in the Hong Kong Polytechnic University and JSPS Fellowship in Nagoya University, he became a professor at FJIRSM in 1998. Now, he is the director of FJIRSM. His main research interests include inorganic-organic hybrid materials, nanomaterials and supramolecular chemistry.

Chin. J. Struct. Chem. **2022**, 41, 2205001-2205014
DOI: 10.14102/j.cnki.0254-5861.2022-0075